Design Optimization of Integrated Rotational Inductor for High-Speed AC Drive Applications

M. Raza Khowja[1], Chris Gerada[1,2], Gaurang Vakil[1], Chintan Patel[1] and Pat Wheeler[1]
[1]Power Electronics, Machine and Control Group, University of Nottingham, Nottingham, UK, Raza.Khowja@nottingham.ac.uk
[2]Power Electronics, Machine and Control Group, University of Nottingham Ningbo, Ningbo, China.

***Abstract*— In order to make an efficient and power dense overall system, a close physical and functional integration of passive components is required instead of having a separate sub-system for passives. Such power dense system is vital in aerospace and marine applications. This paper presents the design optimization of integrated rotational inductors for high speed AC drive applications. Design degrees of freedom like slot-pole combinations along with different winding configurations such as, single layer (SL), double layer (DL), concentrated winding (CW) and distributed winding (DW) are considered. In this paper, the rotational inductors are optimized for these degrees of freedom and compared with a benchmark EE core inductor in terms of total losses, weight and AC copper resistance at both fundamental frequency (1 kHz) and switching frequency (10, 15 and 20 kHz). The comparative analysis between EE core and rotational inductors has shown a significant reduction in total losses and AC copper resistance at fundamental frequency and all switching frequencies. In comparison with EE core inductor, 12 slots 2 poles rotational inductor with SL DW gives lowest total losses at fundamental frequency whereas 6 slots 2 poles rotational inductor with SL DW offers the lowest AC copper resistance at both fundamental and all switching frequencies.**

Keywords*— *EE Core Inductor, Integrated Rotational Inductors, Concentrated winding and Distributed winding.

I. ACRONYMS

DW	Distributed Winding
CW	Concentrated Winding
FSW	Switching Frequency
SL	Single Layer
DL	Double Layer
RT	Rotational
6S	Six Slots
12S	Twelve Slots
18S	Eighteen Slots
2P	Two Poles
4P	Four Poles
6P	Six Poles

II. INTRODUCTION

The passive elements such as filter inductors and capacitors occupy a significant amount of space in motor drives system and have added disadvantage like potential higher weight and losses. In classical motor drives, filters are designed and introduced discretely after the drive system components have been defined. This leads to a separate sub-system which in turn results in a lossy and bulky overall system. In order to overcome these drawbacks the integration of passive components need to be introduced both from functional and physical point of view [1-5].

There are different concepts and considerations in motor drives system to integrate the passive filter components. The integration of passive components in motor drives offer many advantages such as power dense design, reduction in cost, mass, size and shortens the manufacturing process. Thus, applications where high power density is required, integrated options for passives is the most suitable solution [1, 2].

The objective of this paper is to understand the effect of design degrees of freedom on the motor-shaped rotational inductors, proposed in [4], and optimize them for high speed AC drives applications with an aim to reduce losses at both fundamental and switching frequency. Different slot-pole combinations and winding arrangements are considered and compared with a benchmark EE core inductor. From the slot-pole perspective, 6, 12 and 18 slots with 2, 4 and 6 poles are considered. And from the winding perspective, concentrated winding (CW) and distributed winding (DW) with single layer (SL) and double layer (DL) are considered. All designs are modelled and analysed through 2D finite element analysis (FEA). Since the effect of end winding inductance and end winding leakage flux is negligible compared to inductance and the leakage flux of the machine itself, the 3D finite element analysis, which is extremely time consuming and computationally expensive, have not been considered in this paper.

III. LITERATURE REVIEW

Novel integrated options for passive filter inductor which includes: motor-shaped rotational (RT) and rotor-less inductor for high speed AC drives is presented in [4]. Both RT and rotor-less inductor designs are integrated axially, on the same shaft, inside the motor housing and as a result singular shared cooling system can be utilized. As the rotor rotates at the synchronous speeds, iron losses are minimized for the rotational inductor. This makes the rotational inductor most appropriate for the output filter in an inverter fed drives. On the other hand, it is ideal to use the rotor-less inductors as a high power line inductors or an isolation transformers. Furthermore, for the motor-shaped inductors (either rotational or rotor-less) the AC resistance, arising due to proximity effects, is significantly reduced compared to conventional EE core inductor.

In [5], a novel approach to integrate the inverter output filter inductor is presented for PMSM motor drives. The paper

978-1-5090-4281-4/17/$31.00 ©2017 IEEE

uses the existing motor magnetics as a filter inductance instead of using a separate inductor. This leads to the elimination of power losses, weight and space associated with it.

The design of integrated filter inductor for power factor correction application is described in [6]. The stator core laminations are adjusted to increase the stator back iron which act as an integrated filter inductor. This modification increases the stator core outer diameter of the machine.

The complete stator back iron can be used as magnetic component for one or more discrete inductors by integrating toroidal winding which drives alternating magnetic flux in the loops through the back iron of the stator core [7-8].

IV. Inductor Design Methodology

A. Area Product Equation

Referring to Fig. 1 if the inductor current and terminals voltage are sinusoidal, the induced voltage across the inductor terminals according to the Faraday's law is given by,

$$V_{\max} = N\psi_{\max}\omega \tag{1}$$

$$V_{rms} = \frac{2\pi f}{\sqrt{2}} NA_c B_{\max} = k_w NA_c B_{\max} f \tag{2}$$

where k_w is the waveform factor, A_c, ϕ_{max}, B_{max}, f and N are cross-sectional area, magnetic flux, peak operating flux density of the magnetic core, operating frequency and number of turns respectively. The number of turns per phase of the inductor for a given window and conductor strand area can be determined by,

$$N = \frac{k_f W_a}{A_w} \tag{3}$$

where, k_f is the slot fill factor which is defined by the ratio of window area to the copper area. W_a is the window area and A_w is the strand area of conductor.

In practice fill factor is introduced (which varies from 0.4 to 0.6) to provide enough space for bare wire insulation, slot liner and air space between the insulated wire turn. By substituting the Eq. 3 in Eq. 2, we have,

$$V_{rms} = \frac{k_w k_f B_{\max} f A_c W_a}{A_w} \tag{4}$$

Multiplying the RMS current through the inductor on both sides, we have,

$$I_{rms} V_{rms} = \frac{k_w k_f B_{\max} f A_c W_a I_{rms}}{A_w} \tag{5}$$

where, J_{rms} is the RMS current density which is limited by heat losses in the windings. Solving for $W_a.A_c$ we have,

$$W_a A_c = \frac{I_{rms} V_{rms}}{k_w k_f B_{\max} J_{rms} f} \tag{6}$$

Eq. 6 can now be rewritten as,

$$W_a A_c = 2\pi \frac{I_{rms}^2 L_S}{k_w k_f B_{\max} J_{rms}} \tag{7}$$

where L_s is the synchronous inductance of an inductor. For three phase inductor the area product is different from the one indicated in Eq. 6. Since the window utilization is half, the window area is different and the area product changes to,

$$W_a A_c = \frac{1.5 I_{rms} V_{rms}}{k_w k_f B_{\max} J_{rms} f} \tag{8}$$

From Eq. 7, it can be seen that factors, such as flux density, supply frequency, current density and the window fill factor, all have an impact on the inductor's area product. The left-hand side of Eq. 7 indicates the mechanical core parameters, whereas right-hand side shows the electrical parameters of an inductor. The parameter A_c is related to the flux conduction capabilities whereas parameter W_a is related to the current conduction capabilities of an inductor [12].

It is worth noting here that the area product (Eq. 7) does not depends on the supply frequency. However, the core losses strongly depends on it. Therefore, when designing an inductor for very high frequencies (kHz to MHz) it is necessary to select core flux density to a lower values compared to when designing an inductor for low frequencies (Hz to kHz) [11,13].

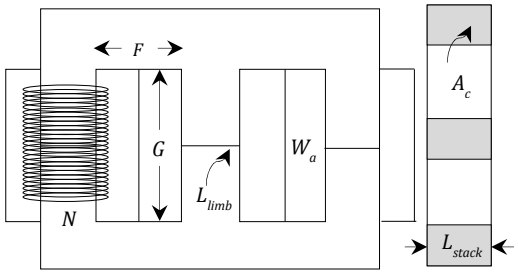

Fig. 1. Layout of 3 Phase EE core Inductor

B. Sizing of EE Core Inductor

To size the EE core inductor area product approach is adopted as stated above. The EE core inductor is sized up by specifying the required inductance, maximum flux density in the core, RMS current, window fill factor, RMS current density and the type of core material, the details of which are shown in Table I.

TABLE I. Inductor Specifications

SPECIFICATIONS	VALUES	UNIT
Magnetic Material	Non Oriented Steel M – 15 29 Ga	-
Required Inductance	1.3	mH
Operating Current	18	A
Operating Frequency	1000	Hz
Switching Frequencies	10, 15 & 20	kHz
Turns per slot	20	-
Slot Fill Factor	0.49	-
Slot Area	2×212	mm-sq
Conductor Diameter	2.6	mm
RMS Current Density	2.36	A/mm^2
Rotaional Inductor Shaft Diameter	27	mm

Once the area product is calculated, the window-to-core area is assumed as 0.25. The window-to-core area ratio (W_a/A_c) indicates a trade-off between core and copper losses. It has been suggested in [12] to set a low window-to-core area ratio in order to keep the fringing flux at minimum level.

The core length ratio (L_{stack}/L_{limb}) and window aspect ratio (G/F) are then considered as 15.5 and 3 in order to set the lengths of the core and window dimensions respectively. The turns per phase are calculated based on the specified voltage across the inductor. In the end, airgap is fixed to get a required inductance of an inductor. So, the number of turns and length of the airgap are given as,

$$N = \frac{V_{rms}}{k_f B_{\max} f A_c} \tag{9}$$

$$L_g = \frac{\left(4\pi\ x10^{-7}\right)N^2 A_c}{L_S} \tag{10}$$

C. Sizing of Rotational Inductor

For the rotational inductor shown in Fig. 2, window area (W_a) is kept same for each slot as that for EE core inductor to have the same inductance effect and electrical loading per slot. The tooth width (Tw) is selected close to the limb length (L_{limb}) of EE core inductor as the core area (A_c) is variable near the tooth. The back iron width (B_w) is adjusted until the flux density becomes equal to the flux density in the teeth. The airgap length (L_g) and the slot opening (S_o) are varied until the required flux density (B_{max}) is reached in the stator teeth and back iron. Finally, the rotor width (R_w) is varied until the same flux density is achieved as that of teeth and back iron.

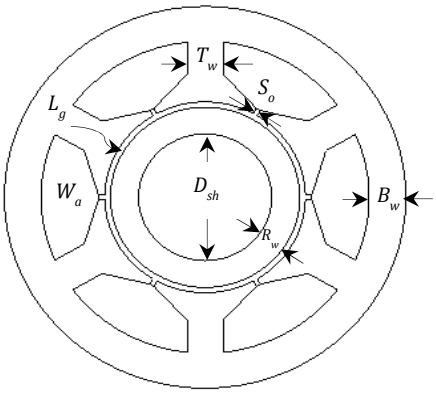

Fig. 2. Layout of 3 Phase 6S Rotational Inductor

V. Integrated Rotational Inductor

The integrated rotational inductor is shown in Fig. 3. The motor-shaped rotational inductor design is extensively different from conventional EE core inductor. It has stator and rotor like conventional motor or generator but without any winding, magnet, or saliency on the rotor. This motor like shape allows the rotational inductor to integrate within the motor or generator by mounting the inductor rotor on the same machine shaft. This allows the inductor and machine to share the same housing and same cooling system. Because the motor-shaped rotational inductor uses the same cooling system as that of motor or generator (compared to no cooling), it can be operated with a higher current densities that would result in to reduced overall size and weight of the inductor.

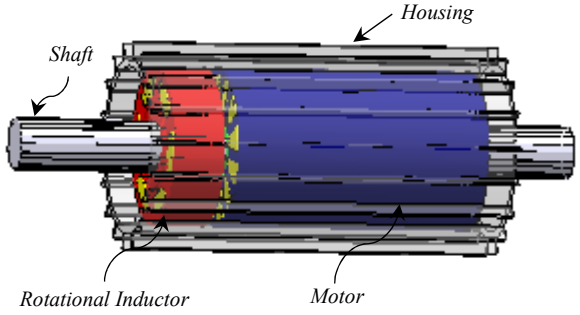

Fig. 3. Integrated Motor-shaped Rotational Inductor

More importantly, the fundamental iron losses in the rotor will be eliminated as the rotor of motor-shaped rotational inductor is rotating at synchronous speed which results in negligible flux variation in rotor. Furthermore, the design of the motor-shaped rotational inductor can be optimized by varying its physical layout such as slot opening, slot opening height, teeth width, teeth height etc.

A. Finite Element Validation of Rotational Inductor

To validate the concept of the rotational inductor, a finite element (FE) model was made in Infolytica MagNet software. The inductor design [5] is considered when the rotor is rotating and standstill. The X and Y components of magnetic flux density in the rotor at one point are evaluated for both static and rotating rotor. The X and Y components of magnetic flux density are then converted into the d-q reference frame. As the q component of the rotor flux density is zero, only the d component of the rotor flux density is shown in Fig. 4.

It can be seen that the flux density in the rotor is not rotating but stationary when the rotor rotates at synchronous speed, and hence minimizes the iron losses in the rotor. However, it contains harmonics due to slotting of the stator. On the other hand, the flux density is varying sinusoidally when the rotor is not rotating.

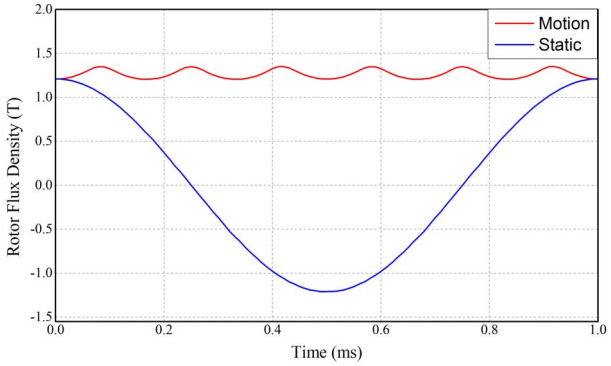

Fig. 4. d-component of flux Density for Static and Rotating Rotor

B. Importance and Applications

Since the rotational inductor is extensively different from conventional EE core inductor it has many applications to use as passive filter inductors or transformers for both low and

high frequencies operation. Rotational inductor is the ultimate choice for high power motor or generator drives where fundamental current and frequency is high so that more losses can be minimized through the rotor magnetic path. However, if the rotor is removed [4], it can be a suitable solution for high power line inductors, isolation and power transformers where supply frequency is fixed and cooling requirement is high. These can then be integrated within the motor or generator housing to share the existing cooling system.

VI. Winding Configurations

Concentrated and distributed windings are the most widely used winding configurations for electrical machines. The CWs are wound together around each tooth to form a complete coil. The length of end winding is shorter for CW compared to that of DW, which leads to lower mean length per turn and thus, reduces the total copper losses [8-9].

However, CW induces lower mutual inductance compared to the DW which reduces the total inductance of the winding. This is due to the short pitching of the coils. The CW also induces harmonic components which lead to an increase in frequency dependent losses in the iron core such as hysteresis and eddy current loss [9]. DW is wound on multiple tooth and distributed throughout the stator periphery in either full-pitch, short-pitch or fractional-pitch arrangement. The DWs are distributed sinusoidal windings which leads to lower space harmonics and hence, lower leakage flux [8].

The windings of a motor or generator can be single or double layer depending on the application of the machine. The cross section view from the side of the machine of end winding length is shown in Fig. 5(a)-(c). The practical implementation of the DW is having end winding length more than the single layer (SL) CW while on the other hand, double layer (DL) CW give the lowest end winding length and hence lowest total copper loss.

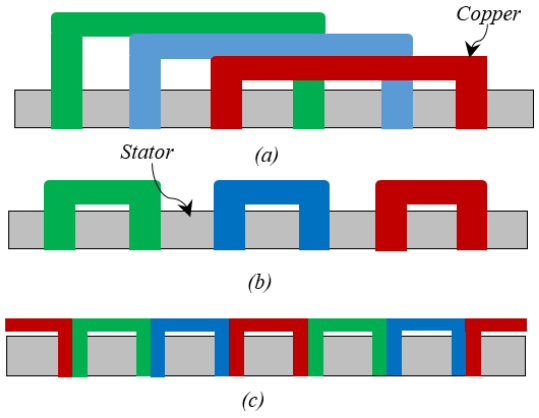

Fig. 5. Side cross section of end winding lengths (a) SL DW (b) SL CW (c) DL CW

VII. Design Optimization Of Motor-Shaped Inductors

A number of integrated motor-shaped rotational inductors were designed with different slot-pole combinations and different winding configuration. The rotational inductors were optimized and compare with conventional EE core inductor in terms of total losses, weight and AC copper loss.

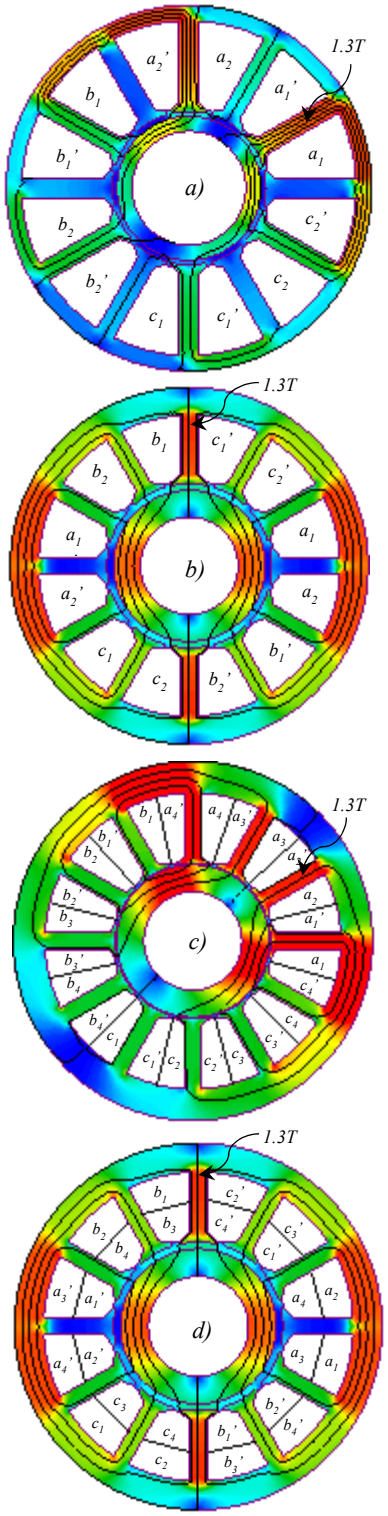

Fig. 6. Winding Configuration of 12 Slots 2 Poles Combination (a) RT CW SL (b) RT DW SL (c) RT SNW DL (d) RT DW DL

EE core inductor is first designed [11] and then converted into motor-shaped rotational inductors [4]. For the purpose of

fair comparison, the type of core material, synchronous inductance, operating flux density, fundamental frequency, switching frequency, turns per slot, slot fill factor, slot area and conductor diameter were kept unchanged and the details of which are provided in Table I.

6, 12 and 18 slots with 2, 4 and 6 poles have been considered in the study. On the other hand, CW and DW with single and double layers were chosen. All designs were modelled and analysed through two dimensional finite element analyses (FEA). The flux distribution plots for different winding layouts of 12 slots and 2 poles rotational inductor are shown in Fig 6(a)-(d).

DC copper losses initially we determined without the end windings and the inductor stack length were kept the same for the EE core inductor and motor-shaped inductors. Since DW gives higher inductance than the CW, the stack length of motor-shaped inductors was changed to keep the synchronous inductance same for all inductor designs. Thus the end turn length was determined by considering an arc of semi-circle, shown in Fig. 7, and included in the DC copper loss calculations to increase the accuracy of the process.

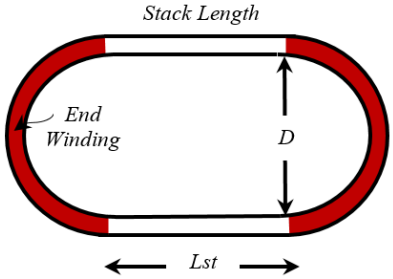

Fig. 7. Single Conductor with End Winding Length

For the calculation of copper loss the total mean length per turn of a conductor is twice the sum of the stack length and the semicircle arc around the corner. The total mean length per turn is given as,

$$MLTP = 2L_{st} + \pi D \tag{11}$$

The comparative analysis between EE core inductor and motor-shaped inductors with different valid slot-pole combination is presented in section IV (A)-(C). Single and double layer CW and DW are considered for each of the slot-pole combination.

A. 2 Poles with 6, 12 and 18 slots Combination

The motor-shaped rotational inductors are analysed and compared with EE core inductor in terms of total losses and total weight. The performance comparison of 2 poles (2P) rotational inductor with 6, 12 and 18 slots combination is presented in Table II. The total losses consist of fundamental iron and copper losses and the total weight consists of stator, rotor and winding weight while considering the inductor end windings.

It can be observed from the Table II that, the DW gives the higher inductance as compared to CW. This is because; the full pitch arrangement of the distributed winding induces higher voltage across it. The short pitch arrangement of the CW resulted in a lower synchronous inductance. Table II also compares the stack length of the rotational inductors which is varied in proportion in order to make the synchronous inductance equal to the targeted value. The synchronous inductance is remain same for SL and DL design since changing from SL to DL does only affect the end winding length of the windings.

TABLE II. PERFORMANCE COMPARSION OF 2 POLES ROTATIONAL INDUCTOR WITH 6, 12 AND 18 SLOTS COMBINATION

	EE Core	RT CW SL	RT DW SL	RT CW DL	RT DW DL
SLOTS	**Total Losses (W)**				
6	151.4	166	119.9	215.4	154.1
12	151.4	146.6	92.6	332.5	92.6
18	151.4	156.2	82.7	362.7	82.7
	Total Weight (Kg)				
6	2.28	2.74	2.39	3.5	2.35
12	2.28	3.53	2.4	4.92	2.44
18	2.28	3.7	3.17	5.9	3.17
	Synchronous Inductance for Stack Length of 114.5mm (mH)				
6	1.3	1.2	2.3	1.2	2.3
12	1.3	1.4	5.1	1.4	5.1
18	1.3	1.8	8.4	1.8	8.4
	Stack Length for 1.3mH Synchronous Inductance (mm)				
6	114.5	124	64.7	124	64.7
12	114.5	106.3	29.2	106.3	29.2
18	114.5	84.6	17.71	84.6	17.71

In comparison with EE inductor, 18 slots is the most efficient combination for 2 poles rotational inductor with SL DW. The total reduction in losses for 18 slots rotational inductor with SL and DL DW are 45.3% when compared with EE core inductor. In general, 12 slots rotational inductor contributes better performance in terms of total losses and weight of the inductor. For 12 slots rotational inductor, the total losses are reduced from 151.4W to 92.6W, i.e. 38.8% reduction, while the total weight inductor is increased by 5.3% compared to EE core inductor due to the full pitch arrangement of the DW.

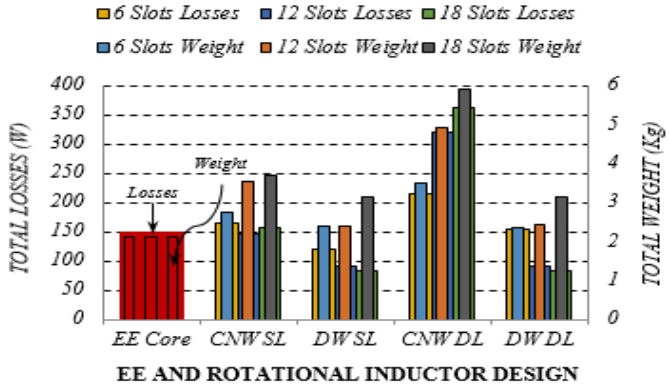

Fig. 8. Comparison of 2 Poles Rotational Inductor with 6, 12 and 18 Slots

Consequently, the CW requires higher stack length to meet the inductance requirement which in turn increases the total losses and weight of the inductor. The comparison of the total

losses and weight between EE and rotational inductor with 6, 12 and 18 slots combination is shown in Fig. 8.

B. 4 Poles with 6, 12 and 18 slots Combination

The performance comparison of 4 poles (4P) rotational inductor with 6, 12 and 18 slots combination is presented in Table III. It can be observed from the Table III that the SL DW gives the higher inductance as compared to SL CW due to different winding arrangements. The DL DW also gives the higher inductance than DL CW in 12 and 18 slots inductors whereas the inductance remain unchanged in DL DW and DL CW for 6 slots inductor.

Table III also compares the stack length of the rotational inductors which is varied in order to make the synchronous inductance equal to the targeted value. The synchronous inductance and hence stack length remain unchanged for SL and DL design.

Compared to the EE core inductor, the most efficient inductor design with 4 poles combination is DL 18 slots rotational inductor with DW. For 18 slots rotational inductor with DL DW, the total losses are reduced from 151.4W to 98.6W, i.e. 35% reduction. The comparison of the total losses and weight between EE and rotational inductor for 6, 12 and 18 slots combination is shown in Table III and Fig. 9.

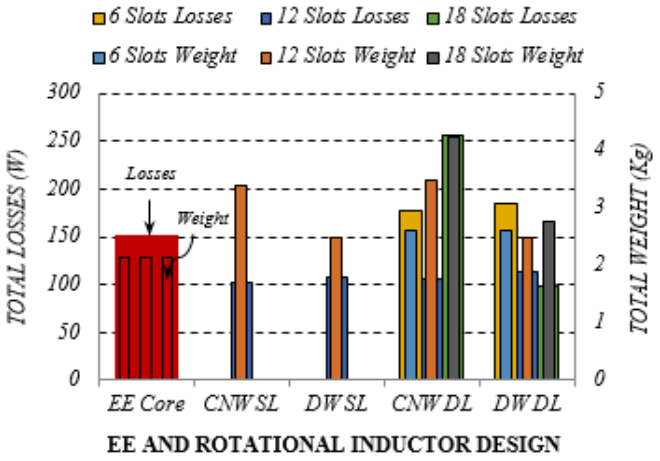

Fig. 9. Comparison of 4 Poles Rotational Inductor with 6, 12 and 18 Slots

C. 6 Poles with 6, 12 and 18 slots Combination

The performance comparison of 6 poles (6P) rotational inductor with only 18 slots is presented in Table IV as the 6 and 12 slots winding are not feasible. It can be seen in Table IV that the SL DW and DL DW gives the higher inductance as compared to SL CW and DL CW. The stack length is changed in accordance with the synchronous inductance. The most efficient design for 6 poles combination is 18 slots with SL DW with relatively higher weight. For 18 slots rotational inductor with DW, the total losses are reduced from 151.4W to 113.7W for SL, i.e. 24.9% reduction, and are reduced from 151.4 W to 114.8 W for DL, i.e. 24.1% reduction. The comparison of the total losses and weight between conventional EE core and rotational inductor with 6, 12 and 18 slot and 6 poles is shown in Table VI and Fig. 10.

TABLE III. PERFORMANCE COMPARISON OF 4 POLES ROTATION INDUCTOR WITH 6, 12 AND 18 SLOTS COMBINATION

	EE Core	RT CW SL	RT DW SL	RT CW DL	RT DW DL
SLOTS	**Total Losses (W)**				
6	151.4	-	-	196.1	197.5
12	151.4	117.3	107.5	105.4	114.5
18	151.4	-	-	257.1	98.4
	Total Weight (Kg)				
6	2.28	-	-	2.31	2.39
12	2.28	3.22	2.5	3.5	2.5
18	2.28	-	-	4.25	2.76
	Synchronous Inductance for Stack Length of 114.5mm (mH)				
6	1.3	-	-	1.16	1.16
12	1.3	1.3	2.56	1.5	2.56
18	1.3	-	-	1.9	4.7
	Stack Length for 1.3mH Synchronous Inductance (mm)				
6	114.5	-	-	128.2	128.2
12	114.5	114.5	57.7	99.2	58.1
18	114.5	-	-	78.3	31.7

TABLE IV. PERFORMANCE COMPARISON OF 6 POLES ROTATION INDUCTOR WITH 18 SLOTS COMBINATION

PARAMETERS	EE Core	RT CW SL	RT DW SL	RT CW DL	RT DW DL
Total Losses (W)	151.4	139.1	113.7	218.4	114.8
Total Weight (Kg)	2.28	3.71	2.78	3.91	2.87
Synchronous Inductance for Stack Length of 114.5mm (mH)	1.3	1.5	2.97	1.48	2.88
Stack Length for 1.3mH Synchronous Inductance (mm)	114.5	99.2	50.5	100.6	51.7

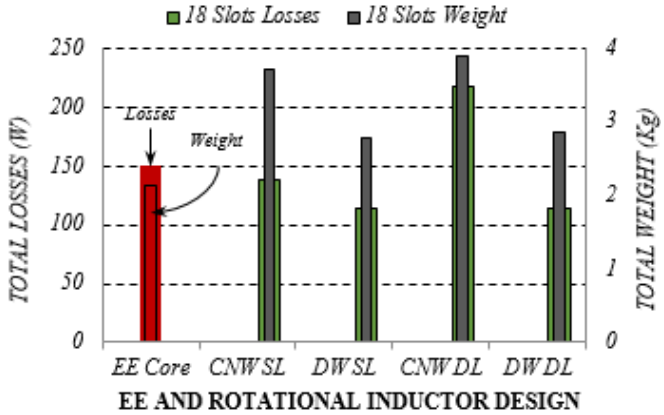

Fig. 10. Comparison of 6 Poles Rotational Inductor with 6, 12 and 18 Slots

D. Comparsion of AC Loss

The best inductor designs were selected from the performance comparison of rotational inductors for different pole combinations and their AC copper loss were analysed and

compared with EE core inductor. One inductor design has been selected from each of the pole and slot column. The selected inductor designs are: 6 slots (6S) 2P DW SL, 12 slots (12S) 2P DW SL, 18 slots (18S) 2P DW SL, 12S 4P DW SL and 18S 6P DW SL.

Solid conductors were modelled to evaluate AC copper loss at fundamental and switching frequency (FSW). The current densities of selected inductor designs, when phase 'a' reaches its peak value are shown in Fig. 11(a)-(f). The magnitude of the harmonic component is considered to be 5% of fundamental for determining and analysing AC copper loss. The fundamental current with switching frequency components were injected into the FEA model.

The injected current equations are shown in Eq. 12 to Eq. 14 for 10kHz, 15kHz and 20kHz respectively where '*w*' represents the angular fundamental frequency which is 6.28*1000 rad/sec.

$$i_{10khz} = 18.[Sin(\omega t) + 0.05Sin(10\omega t)] \quad (12)$$

$$i_{15khz} = 18.[Sin(\omega t) + 0.05Sin(15\omega t)] \quad (13)$$

$$i_{20khz} = 18.[Sin(\omega t) + 0.05Sin(20\omega t)] \quad (14)$$

The relation between DC and AC copper loss is given by,

$$P_{copper} = P_{ac} + P_{dc} \quad (15)$$

where, P_{copper} is the total copper losses, P_{dc} is the DC copper loss with end winding effect taking into account and P_{ac} is the AC copper loss due to skin and proximity effect where end winding AC copper loss effect is neglected.

The AC copper loss in the conventional EE core inductor is found to be higher than that of rotational inductors with 2P combination at fundamental and all considered switching frequencies, and is shown in Table V. Rotational inductor with 6S and SL DW gives the lowest AC copper loss at both fundamental frequency and switching frequencies of 10, 15 and 20 kHz amongst all.

For rotational inductor with 6S 2P SL DW, the AC copper loss reduction of 72.04% is achieved at fundamental frequency, whereas the reduction of 74.14%, 74.13 and 74.12% is achieved at all switching frequencies respectively compared to the conventional EE core inductor. Rotational inductor with 12S 4P SL DW provides the reduction of 53.43% at fundamental frequency, whereas the reduction of 58.26%, 59.25 and 59.93% is obtained at all considered switching frequencies respectively.

Rotational inductor with 18S 2P SL DW is unable to provide high AC copper loss reduction due to higher leakage and fringing fluxes around the stator slots opening. This is due to the increase in the number of turns per phase as the number of turns per slot kept constant for all inductor designs.

It is important to note that most of the conductors are placed close to the airgap in EE design which would be exposed to increased flux cutting them due to fringing effect. In contrast, conductors of rotational inductors are placed far

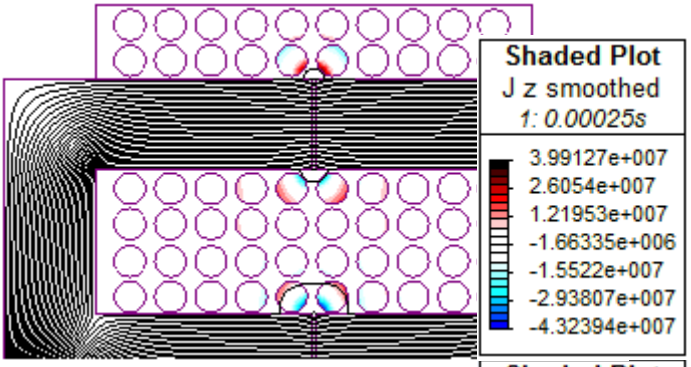

a)

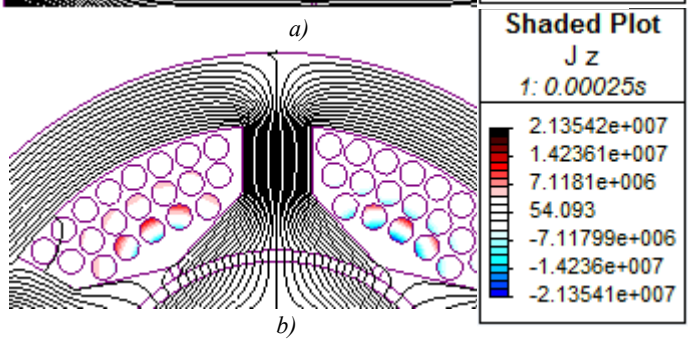

b)

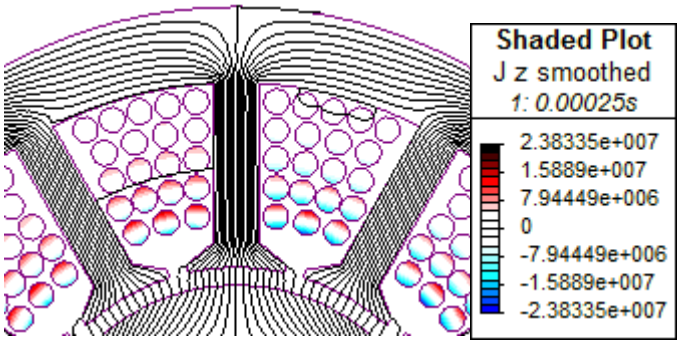

c)

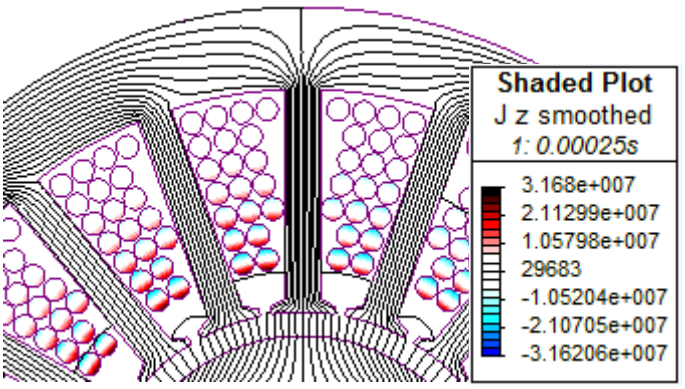

d)

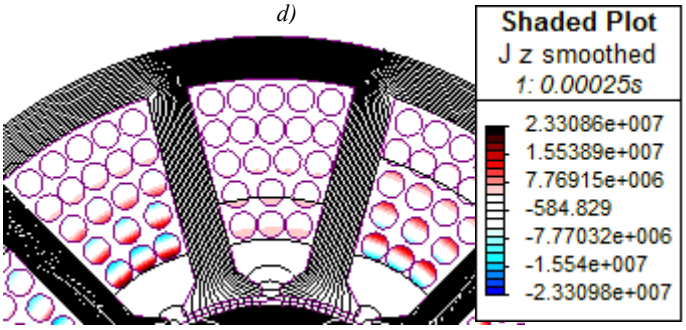

e)

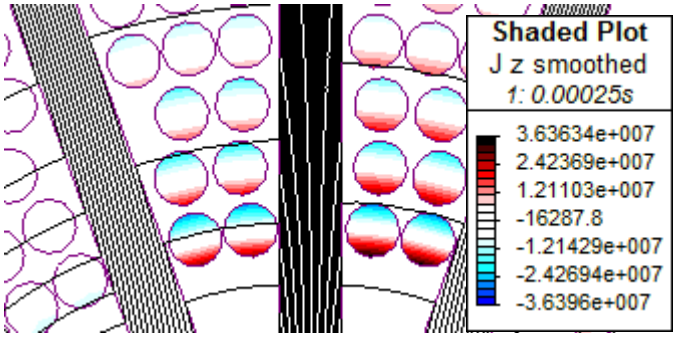

f)

Fig. 11. Effect of Leakage and Fringing Flux at 1000 Hz for EE and Rotational Inductors (a) EE Core (b) 2P 6S DW SL (c) 2P 12S DW SL (d) 2P 18S DW SL (e) 4P 12S DW SL (f) 6P 18S DW SL

from the slot opening or airgap and therefore, experiences less fringing flux. The effect of leakage flux is likewise lesser in the rotational inductors with 2P combination as its slot width is wider than the window width of the EE inductor. The effect of fringing and leakage fluxes are responsible for increased flux cutting the conductors in EE core inductor thus increasing the AC resistance, and hence, AC copper losses at both fundamental and all switching frequencies.

For 4P rotational inductor with SL DW, the AC copper loss reduction at fundamental frequency is 2.78% and 5.83%, 8.5% and 10.33 at all considered switching frequencies respectively, whereas the AC copper loss are increased more than twice for 6P rotational inductors, when compared to the conventional EE core inductor. This is because the flux path for 4P and 6P inductors is smaller than the 2P inductor which has increased the effect of leakage flux through the stator slots.

TABLE V. COMPARISON OF AC COPPER LOSS

FSW (kHz)	EE Core	6S 2P DW SL	12S 2P DW SL	18S 2P DW SL	12S 4P DW SL	18S 6P DW SL	UNITS
1	17.49	4.89	8.15	15.39	17.00	53.23	W
10	1.42	0.37	0.59	1.12	1.33	3.77	W
15	1.98	0.51	0.81	1.53	1.81	5.45	W
20	2.47	0.64	0.99	1.89	2.21	6.87	W

VIII. CONCLUSIONS

A number of integrated rotational inductors were designed and proposed in this paper with different slot-pole combinations. The single and double layer concentrated and distributed winding were chosen. The rotational inductors were optimized and then compared with EE core inductor in terms of total losses, weight and AC resistance at fundamental and all considered switching frequencies.

The comparative analysis between EE core and rotational inductors has shown a significant reduction in total losses and AC resistance at both fundamental and switching frequencies. For 12 slots 2 poles rotational inductor with SL DW, the total losses at fundamental frequency was reduced by 39% when compared to EE core inductor. This comes at the expense of 5.2% increase in weight. For 18 slots 4 poles rotational inductor with DL DW, the total losses at fundamental frequency was reduced by 35% when compared to EE core inductor. This comes at the expense of 21.1% increase in weight. For 18 slots 6 poles rotational inductor with SL DW, the total losses at fundamental frequency was reduced by 24.9% when compared to EE core inductor. This comes at the expense of 21.9% increase in weight.

Moreover, the AC loss at fundamental and all switching frequencies were reduced dramatically when compared with EE core inductor. 6S rotational inductor with SL DW contributed the lowest AC copper loss at both fundamental frequency and switching frequencies of 10, 15 and 20 kHz amongst all the inductor design. For 6S 2P SL DW, the AC loss reduction of 72.04% was achieved at fundamental frequency, whereas the reduction of 74.14%, 74.13 and 74.12% is achieved at all switching frequencies respectively, when compared with the EE core inductor. 12S 4P rotational inductor with SL DW offered the reduction of 53.43% at fundamental frequency, whereas the reduction of 58.26%, 59.25 and 59.93% was achieved at all considered switching frequencies respectively.

REFERENCES

[1] Robert Abebe, Gaurang Vakil, Giovanni Lo Calzo, Thmas Cox, Simon Lambert, Mark Johnson, Chris Gerada, Barrie Mecrow "Integrated motor drives: state of the art and future trends" IET Electric Power Applications, 15 pp, Print ISSN 1751-8660, Online ISSN 1751-8679

[2] Popovic-Gerber Jelena, Gerber M, Ferreira Braham "Integrated filter in electrolytic capacitor technology for implementation in high power density idustrial drives" Power Electronics Specialists Conference, 2008. PESC 2008. IEEE. Publication Year: 2008 , Page(s): 2968 - 2974

[3] Popovic J, Ferreira J.A, Gerber M.B, Konig A, de Doncker, R. "Integration technologies for high power density power electronic converters for AC drives". Power Electronics, Electrical Drives, Automation and Motion, 2006. SPEEDAM 2006. Publication Year: 2006 , Page(s): 634 – 639

[4] M. Raza Khowja, C. Gerada, G. Vakil, P. Wheeler and C. Patel "Novel Itegraive Options for Passive Filter Inductor in High Speed AC Drives" Industrial Electronics Society, IECON 2016 – 42nd Annual Conference of IEEE

[5] M. Raza Khowja, C. Gerada, G. Vakil, P. Wheeler and C. Patel "Integrated Output Filter Inductor for Permanent Magnet Motor Drives" Industrial Electronics Society, IECON 2016 – 42nd Annual Conference of IEEE

[6] Nee B.M, Chapman P.L. "Integrated Filter Element in Electric Drives" Vehicle Power and Propulsion Conference, 2007. VPPC 2007. IEEE. Publication Year: 2007 , Page(s): 148 - 153

[7] Garvey S.D. Norris, W.T, Wright M.T. "The role of integrated components in protecting motor windings". Electric Power Applications, IEEE Proceedings - Volume: 147 , Issue: 5 Publication Year: 2000

[8] Nakajima, Yuki Imazu, Tomoya Mizukoshi, Yukio Sato, Sho Zushi, Yusuke "Integrated Capacitor Type Stator", Patent No. 8049383

[9] Adam Walker, Micheal Galea, Chris Gerada, Abdeslam Mebarki, David Gerada "Design Considerations for High Performance Traction Machines: Aiming for the FreedomCar 2020 Targets" 2015 International Conference on Electrical Systems for Aircraft, Railway, Ship Propulsion and Road Vehicles (ESARS). Year: 2015 Pages: 1-6

[10] Lester Chong, Rukmi Dutta, Nguyen Quang Dai, M. F. Rahman, Howard Lovatt "Comparison of Concentrated and Distributed Windings in an IPM Machine for Field Weakening Applications" Universities Power Engineering Conference (AUPEC), 2010 20th Australasian. Year: 2010 Pages: 1-5

[11] Kazimierczuk M.K, Sekiya H. "Design of AC resonant inductors using area product method" Energy Conversion Congress and Exposition, 2009. ECCE 2009. IEEE Publication Year: 2009

[12] Colonel Wm. T. McLyman. "Transformer and Inductor Design Handbook" Thrid Edition

[13] H. Nijende, N. Frohleke and J. Bocker, "Optimized size design of integrated magnetic components using area product approach," 2005 European Conference on Power Electronics and Applications, Dresden, 2005, pp. 10 pp.-P.10.